SCISPACE
formerly Typeset

Open access • Journal Article • DOI:10.1051/RPHYSAP:019880023030023900

Creep of SiC-Whisker reinforced Si3N4 — Source link

M. Backhaus-Ricoult, J. Castaing, J.L. Routbort

Institutions: Centre national de la recherche scientifique, Argonne National Laboratory

Published on: 01 Mar 1988

Topics: Diffusion creep, Creep, Grain boundary, Deformation (engineering) and Strain hardening exponent

Related papers:

- SI3N4-SiC composites
- Steady-state creep of hot-pressed SiC whisker-reinforced silicon nitride
- Toughening Behavior in Sic-Whisker-Reinforced Alumina
- Creep Deformation of an Alumina Matrix Composite Reinforced with Silicon Carbide Whiskers
- Hot-pressed SiC whisker/Si3N4 matrix composites

Share this paper:

View more about this paper here: https://typeset.io/papers/creep-of-sic-whisker-reinforced-si3n4-2d7q9ah9vd

Creep of SiC-Whisker reinforced Si3N4

M. Backhaus-Ricoult, J. Castaing, J.L. Routbort

▶ **To cite this version:**

M. Backhaus-Ricoult, J. Castaing, J.L. Routbort. Creep of SiC-Whisker reinforced Si3N4. Revue de Physique Appliquée, Société française de physique / EDP, 1988, 23 (3), pp.239-249. 10.1051/rphysap:01988002303023900 . jpa-00245766

HAL Id: jpa-00245766

https://hal.archives-ouvertes.fr/jpa-00245766

Submitted on 1 Jan 1988

HAL is a multi-disciplinary open access archive for the deposit and dissemination of scientific research documents, whether they are published or not. The documents may come from teaching and research institutions in France or abroad, or from public or private research centers.

L'archive ouverte pluridisciplinaire **HAL**, est destinée au dépôt et à la diffusion de documents scientifiques de niveau recherche, publiés ou non, émanant des établissements d'enseignement et de recherche français ou étrangers, des laboratoires publics ou privés.

Revue Phys. Appl. **23** (1988) 239-249 MARS **1988**, PAGE 239

Classification
Physics Abstracts
62.20 — 81.40

Creep of SiC-Whisker reinforced Si_3N_4

M. Backhaus-Ricoult [1], J. Castaing [1] and J. L. Routbort [2]

[1] CNRS, Laboratoire Physique des Matériaux, 92195 Meudon Cedex, France
[2] Materials Science Division, Argonne National Laboratory, Argonne, U.S.A.

(Reçu le 27 octobre 1987, accepté le 22 décembre 1987)

Résumé. — Le comportement mécanique d'un composite de Si_3N_4 (avec 3 % MgO) contenant de 0 à 20 % de fibres de SiC est étudié par des essais de fluage en compression (100-300 MPa) entre 1 250 et 1 500 °C. Les fibres de SiC n'influencent pas le comportement du fluage jusqu'à des déformations de l'ordre de 0,05. On peut distinguer deux régimes de fluage : un régime à haute température où la déformation se fait à vitesse quasi constante. A basse température la vitesse de déformation diminue rapidement à cause d'un coefficient de durcissement beaucoup plus élevé qu'à haute température. La microstructure des échantillons non-déformés et déformés révèle que les dislocations jouent un rôle négligeable dans les conditions de déformation décrites. Les cavités observées aux points triples et les fissures aux joints de grains et aux interfaces entre matrice et fibres indiquent plutôt un mécanisme de déformation par cavitation et microfissuration.

Abstract. — The mechanical behaviour of a composite of Si_3N_4 (with 3 % MgO) containing 0-20 % SiC whiskers has been investigated by compressive creep experiments (100-300 MPa) at temperatures between 1 250 °C and 1 500 °C. No significant influence of the SiC whiskers on the creep behaviour could be detected up to about 5 % of strain. Two temperature regions could be identified : a) at high temperature the creep deformation occurs at a quasiconstant strain rate. Extended cavitation in the triple junctions occurs. b) At low temperatures, creep rates rapidly decrease due to a strain hardening coefficient much more important than for higher temperatures. In the microstructure, cavities and microcracks along grain boundaries and fiber-matrix interfaces were observed. Dislocations play an insignificant role for the deformation in both temperatures regions.

1. Introduction.

Additive containing hot-pressed or sintered silicon nitride (Si_3N_4) has been recognized as a potential candidate for structural applications at high temperatures because of its low thermal expansion, its good resistance to oxidation and its high strength. However, at high temperatures the strength of these materials degrades [1] due to the presence of a glassy grain boundary phase [2-5]. This grain boundary film can be more or less extended in the differently fluxed materials and is specially broad with Y_2O_3, Al_2O_3 additives. In contrast, the intergranular layer observed in the Mg-doped materials under reducing atmosphere is relatively narrow (< 1 nm) [2, 3] and most of the glass phase is located in triple point pockets. Due to the presence of the liquid film, grain boundary sliding and grain separation occur easily during deformation. Depending on composition and temperature the grain boundary sliding can be accomodated by different mechanisms [6, 7] : elastic deformation of grain boundary asperities and adjacent grains (viscoelastic creep), material transport by diffusion through the bulk or along grain boundaries (diffusional creep : Nabarro Herring or Coble Creep), plastic deformation of adjacent grains by dislocation movement and/or twinning and cavity formation. Cavitation of the liquid film occurs in grain boundaries, particularly at triple junctions due to the large tensile stresses produced by the sliding and the negative pressure in the fluid at these locations [9]. If at low temperatures the glassy phase is brittle, extended cavitation can even yield to the growth of microcracks and, consequently, to easy fracture of the material [10].

Since whisker reinforcement can result in improved properties [11], SiC whiskers produced by a vapour-solid-liquid (VSL) process [12] or commer-

Article published online by EDP Sciences and available at http://dx.doi.org/10.1051/rphysap:01988002303023900

cial SiC whiskers [13] were added to hot pressed MgO-doped Si_3N_4. Indeed, the fracture toughness increases [13] probably due to micro-cracking in the fiber-matrix interfaces. On the other hand, the room-temperature strength of the VSL-whisker reinforced Si_3N_4 decreased with increasing whiskers loading [11] while only a modest improvement in room-temperature strength was achieved with the commercial whiskers [13].

Understanding the high-temperature deformation of these composites is necessary before their incorporation into a structure. Limited creep studies have been performed on SiC-reinforced Al_2O_3 [14] and SiC-whiskers reinforced hot-pressed Si_3N_4 (containing 1.5 wt % Al_2O_3 and 6 wt % Y_2O_3) [15]. In the case of the Al_2O_3 composite, the creep resistance was increased at 1 500 °C and the mode of deformation also changed [14]. Creep studies in SiC-whisker reinforced Si_3N_4 indicate a complex behaviour with a scatter of the observed creep strength in relation to pure Si_3N_4 [15].

The objective of this investigation was to determine the high temperature creep behaviour of a composite, varying the amount of whisker content. For this purpose constant load creep experiments combined with scanning electron microscopy (SEM) and transmission electron microscopy (TEM) were performed on hot-pressed Si_3N_4, to which 3 wt % MgO was added as a sintering aid, containing between 0 and 20 wt % SiC whiskers.

2. Experimental procedures.

2.1 MATERIALS PREPARATION. — The SiC-whiskers-reinforced Si_3N_4 composites were supplied by the Advanced Composite Materials Corporation, Green, South Carolina. The fabrication procedures have been described in [13]. Briefly, the samples were hot-pressed from commercial Si_3N_4 powder to which 3 wt % MgO and the desired amount (0, 5, 10, 20 wt %) of SiC whiskers (~ 0.1-1 μm in diameter and 10-30 μm long) were added and blended. Hot-pressing was performed in a N_2 atmosphere at 1 720-1 750 °C. X-ray diffraction indicated that the samples consisted of primarily β-Si_3N_4 with less than 5 % α-phase. Samples whose dimensions were $4 \times 2 \times 2$ mm were cut from the hot-pressed discs, ground parallel and polished with diamond paste.

An optical micrograph of the starting material with 10 % SiC is given in figure 4.

2.2 EXPERIMENTAL TECHNIQUES. — Samples were crept in a nitrogen atmosphere using a constant compressive load creep machine [16]. The same material as the observed sample was used as the platens. Total dimensional changes were measured by Linear Differential Transformers, but whenever possible, the final dimensions of the sample were used to calculate the sample strain. No correction for the barreling that was generally present was made. The deformed samples were cooled down under stress.

Deformed and undeformed samples were cut parallel and perpendicular to the deformation direction into slices of $2 \times 2 \times 1/2$ mm. For examination in the optical microscope and the SEM these slices were polished with diamond paste (20, 8, 4, 2 μm). Furthermore, some deformed and undeformed samples were notched and then fractured at room temperature. They were observed by SEM to compare the morphology, the grain size distribution and the fiber location before and after deformation.

For TEM thin foils were prepared by further grinding and polishing the sliced disks to a thickness of 30-40 μm. These thin platelets were then ion-thinned until a hole appeared, cemented on copper grids and coated with a thin deposit of carbon to prevent charging in the microscope. The transparent regions of the samples were examined with a Jeol electron microscope operated at 100 KV or with a Philips scanning transmission elctron microscope (STEM) equipped with an energy dispersive X-ray detector (EDX) and an electron energy loss spectrometer (EELS).

3. Results.

3.1 CREEP EXPERIMENTS. — The results of the creep experiments performed at $\approx$ 1 300 °C for stresses between 139 and 150 MPa, are presented in figure 1 in which the logarithm of the strain rate $\dot{\varepsilon}$ is plotted as a function of a true strain, ε. In a constant load creep test, steady state is represented by a straight line, if $\dot{\varepsilon}$ is proportional to σ^n (σ = stress, n = stress exponent). The data plotted in the figure do not begin at $\varepsilon = 0$, because most experiments were preceeded by creep at various lower stresses giving value of $\dot{\varepsilon}$ too low to be included. There is very little difference (within experimental error) in strain rate among the Si_3N_4 and the 10-20 % SiC reinforced Si_3N_4. It is noted, that the data obtained on one of the Si_3N_4 samples in figure 1 have been uncorrected for strain (subtracting the strain due to indentation of the platens) because of specimen fracture. Any correction would move the curve in better accord to the other results. All curves obtained at 1 300 °C indicate a very high strain hardening, $\partial \ln \dot{\varepsilon}/\partial \varepsilon$, between 196 and 352, with an average of 265 ± 70. Data acquired at T = 1 440-1 450 °C and $\sigma \approx 280$ MPa are illustrated in figure 2. Again, as was observed for T = 1 300 °C, there is not effect of the SiC whisker reinforcement on the strain rate, there being only a 30 % difference between the fastest and slowest $\dot{\varepsilon}$. These curves have a much lower strain hardening than those obtained at 1 300 °C, between 16 and 30 with an average of

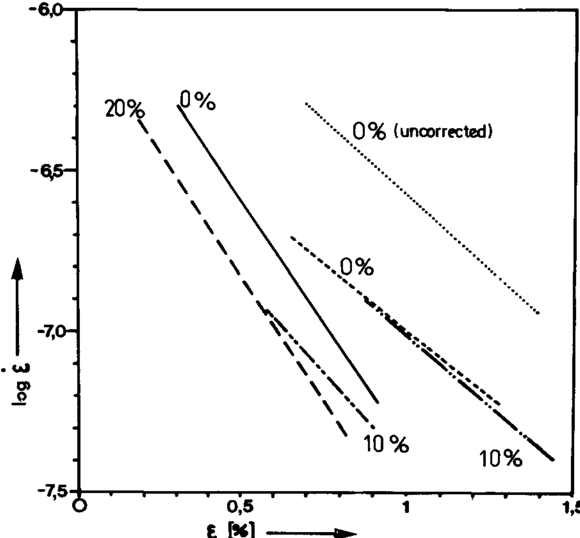

Fig. 1. — Creep of SiC whiskers reinforced Si_3N_4 for $T = 1\,290\text{-}1\,300$ °C and $\sigma = 139\text{-}150$ MPa, $\sigma = F/S_0$ (F = load, S_0 = initial cross section area of the specimen). The data are corrected for sample strain except where indicated. The creep rate $\dot{\varepsilon}$ is in s^{-1}. It is plotted as log $\dot{\varepsilon}$ *versus* strain.

———	10 % SiC, 139 MPa, 1 300 °C (Exp 3)
————	0 % SiC, 141 MPa, 1 300 °C (Exp 4)
----------	20 % SiC, 139 MPa, 1 300 °C (Exp 5)
....	0 % SiC, 139 MPa, 1 300 °C (Exp 6)
----------	0 % SiC, 139 MPa, 1 290 °C (Exp 9)
—·—·—	10 % SiC, 150 MPa, 1 290 °C (Exp 10).

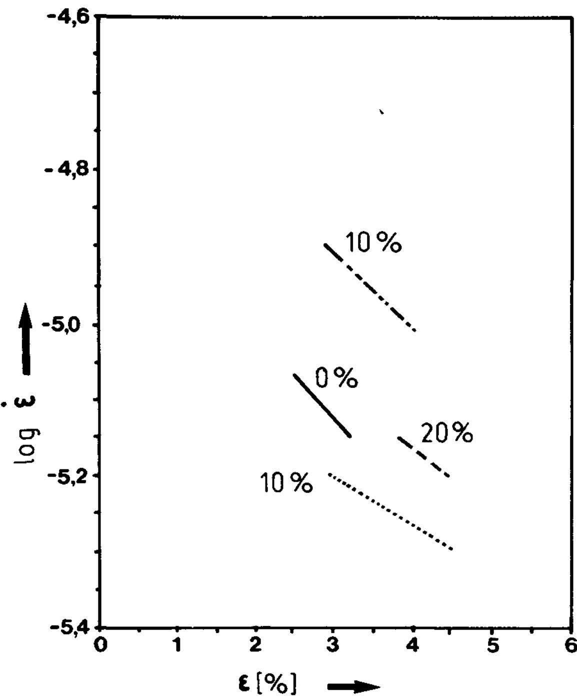

Fig. 2. — Creep of SiC whiskers reinforced Si_3N_4 for $T = 1\,440\text{-}1\,450$ °C and $\sigma = 279\text{-}284$ MPa (the data are corrected for sample strain).

———	10 % SiC, 284 MPa, 1 440 °C (Exp 3)
————	0 % SiC, 281 MPa, 1 440 °C (Exp 4)
----------	20 % SiC, 279 MPa, 1 450 °C (Exp 5)
....	10 % SiC, 280 MPa, 1 440 °C (Exp 11).

21 ± 6. Creep measured at 1 370 °C resulted in a strain hardening of 21 to 48 with an average of 39 ± 10. Therefore, there is an indication that the strain hardening decreases with increasing temperature.

That the strain hardening is primarily a function of temperature and not strain is shown in figure 3. In this experiment performed at $\sigma = 218$ MPa on a Si_3N_4 + 5 wt % SiC sample, the temperature was changed from 1 370 °C to 1 300 °C after more than 2 % strain. The strain hardening increased from 46 to 160.

A summary of the creep parameters is presented in table I. The values of the stress exponent, n, and the activation energy, Q, were determined from stress and temperature changes, respectively. The stress exponents were determined at 1 300 °C and 1 440-1 450 °C, respectively, while Q was measured between 1 300 and 1 450 °C. The fact that the strain hardening coefficient and the stress exponent are not equal indicates that there is some strain hardening. At high temperatures a quasi steady state is reached, but at low temperatures a large strain hardening occurs.

The accumulated data support the suggestion that there are two creep regimes : the large stress exponent being associated with lower temperatures and

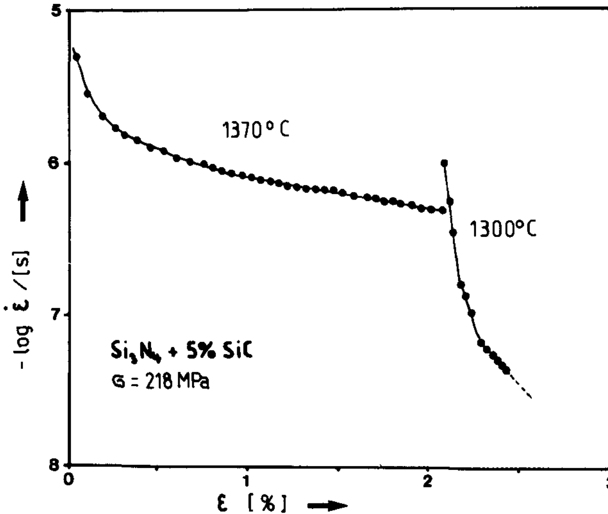

Fig. 3. — log $\dot{\varepsilon}$ *versus* ε for a Si_3N_4 reinforced with 5 wt % SiC for $\sigma = 21.8$ MPa and $T = 1\,370$ °C and 1 300 °C.

higher strain hardening and the lower n occurring at higher temperatures and in conjunction with a low strain hardening.

Statistically there is little difference in n and Q for Si_3N_4 and the various compositions of SiC + Si_3N_4. The stress exponents at 1 300 °C and at 1 440-

Table I. — *Formal creep parameter for equation* $\dot{\varepsilon} = A \cdot \sigma^n e^{-(Q/kT)}$ *($\dot{\varepsilon}$-deformation rate, A-constant, σ-stress, n-stress exponent, Q-activation energy, k-Bolhmann constant, T-temperature) (The errors indicate the experimental scattering).*

wt % SiC	T = 1 300 °C		T = 1 450 °C	
	n	Q[eV/atom]	n	Q[eV/atom]
0	4.3 ± 0.6	8.3 ± 0.5	2.1 ± 0.3	7.4 ± 1.4
10	3.3 ± 0.3	9.1 ± 0.7	1.7	8.4
20	3.5	7.9	2.5	7.3

1 450 °C are 3.6 ± 0.5 and 2.1 + 0.4, respectively, while the low and high temperature values of Q are similar and scatter between 7 and 9 eV/atom. In some experiments of whiskers reinforced Si_3N_4 $\dot{\varepsilon}$ increased by 50 % when the load was removed and reapplied after a 1 h anneal. At the same temperature of 1 450 °C the $\dot{\varepsilon}$ for a pure Si_3N_4 continued after such a removal of the load as if the test was uninterrupted. This effect of recovery and the influence of the fiber-content on the recovery were not further studied.

3.2 MICROSTRUCTURAL OBSERVATIONS. — In the optical microscope the starting material generally appears perfectly dense and in the case of SiC addition the fibers are homogeneously distributed (Fig. 4), but preferentially oriented due to the hot-pressing process. During the processing the average fiber length has largely decreased ! Occasionally, large flaws and, at high SiC content low density agglomerations of fibers can be detected. These extended defects which could easily degrade the material strength could probably be avoided by more careful processing.

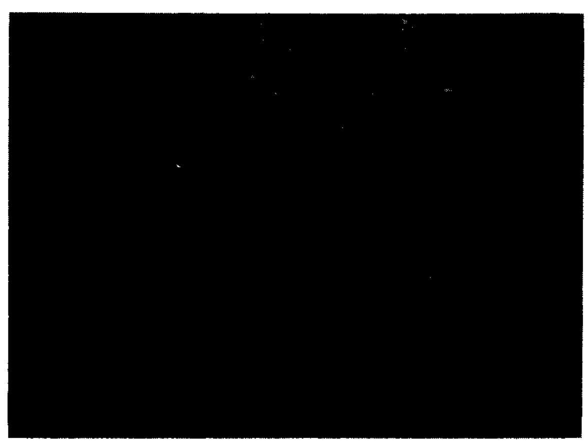

Fig. 4. — Optical micrograph of a non deformed Si_3N_4 reinforced with 15 vol % SiC whiskers (the marker corresponds to 10 μm).

Figure 5 is a typical TEM micrograph of a undeformed Si_3N_4. The morphology of the sample is very inhomogeneous, varying from about 50 nm to 1 μm in grain size and from regular hexagons to heavily deformed hexagons (due to liquid phase sintering) and to bar-like grains. In some triple junctions an intergranular phase could be detected, figure 6, while other triple junctions appear perfectly clean.

Fig. 5. — TEM micrograph (bright field image) of non deformed Si_3N_4. (the marker corresponds to 1 μm).

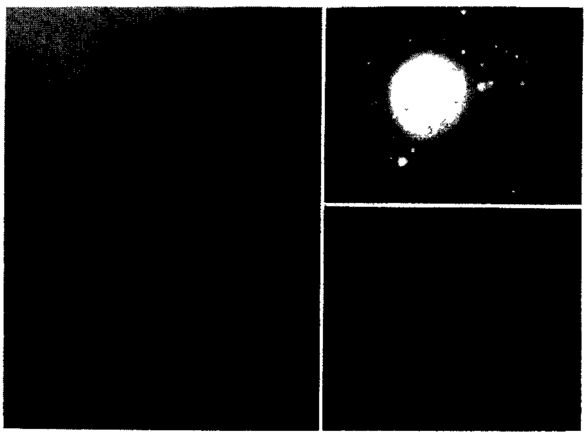

Fig. 6. — Triple junction in non deformed pure Si_3N_4 with an intergranular amorphous phase : a) bright field image (the marker corresponds to 50 nm). b) selected area diffraction pattern on the triple point region, camera length 95 cm. c) dark field image with the weak ring, which is marked in b).

The amorphous character of this intergranular phase was shown by imaging it in dark field condition (Fig. 6b), placing the objective aperture on the ring of diffuse intensity visible in the diffraction pattern of this area (Fig. 6c).

Electron Energy Loss Spectroscopy of the pockets (Fig. 7b) yields the characteristic edges of Si, Mg, O

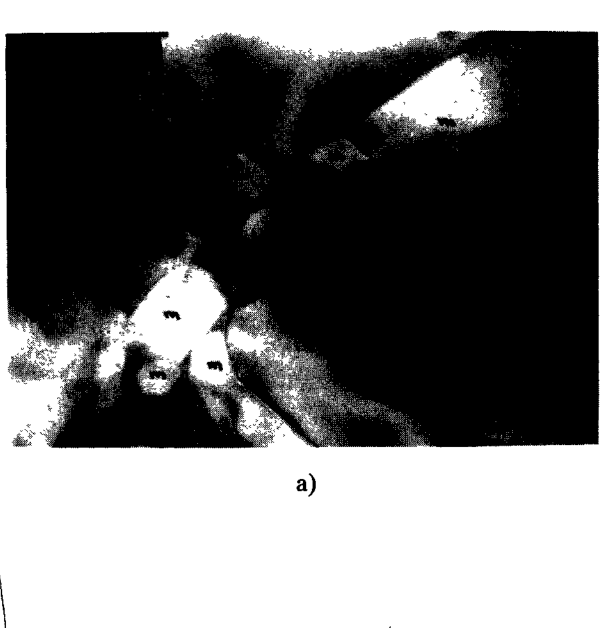

a)

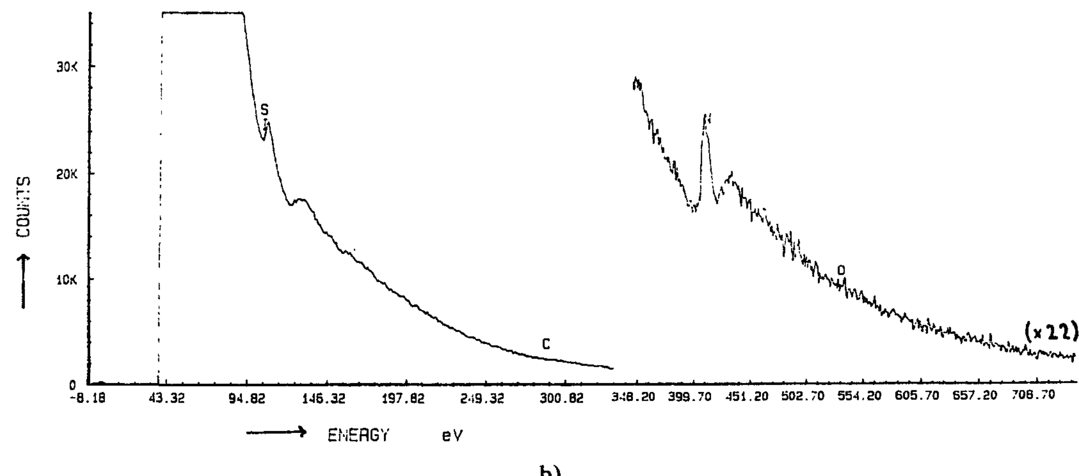

b)

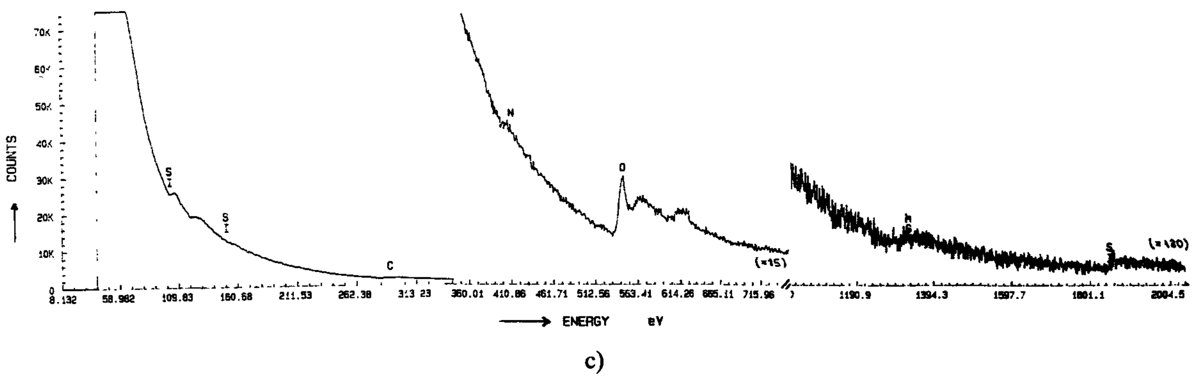

c)

Fig. 7. — Electron energy loss spectra of matrix grains (m) and of triple point pockets (p) : a) bright field image with analysed regions marked by m and p (the marker corresponds to 200 nm). b) spectrum of matrix regions (m). c) spectrum of glassy pockets (p).

and N. This nitrogen edge has a very low intensity and is probably due to the surrounding grains or to small Si_3N_4 nuclei within the pockets. It is reasonable to conclude that the composition of the glassy phase is Mg_2SiO_4, while the surrounding grains are free of oxygen and magnesium (Fig. 7c).

Already the starting material is not dislocation-free, because of localized stresses during hot-pressing.

Addition of SiC whiskers does not change the general appearance of the material. The perfect density is conserved, the fibers are perfectly embedded in the matrix material (Fig. 8). As can be seen in figure 8, the fibers themselves are heavily faulted. In

Fig. 8. — Bright field (BF) image of the non deformed material containing 10 % of SiC whiskers (the marker corresponds to 200 nm).

the interface boundary between SiC and Si_3N_4 no amorphous interface layer or diffusion zone could be detected by analysis and by traditional imaging and microdiffraction techniques in the electron microscope. Lattice imaging might have revealed atomic layers of another phase, but this technique was not available for our studies.

After deformation, a common characteristic structure is present in all samples : areas of several microns (sometimes elongated in one direction), where single grains are separated by a whole system of pores. Sometimes large pores are filled with very small (< 50 nm) grains, which can be regular hexagons or round particles. This typical structure (Fig. 9) will be referred to as « low density pockets » in the following.

Fig. 9. — BF image of a low density pocket in a deformed sample containing 10 % SiC (deformed at 1 290 °C, σ = 250 MPa, $\varepsilon_{total} = 2$ %) (marker : 200 nm).

It was verified by EELS that the grains of these areas were still pure Si_3N_4. Even for the smallest grains in the pockets no oxygen or magnesium could be detected (which excludes that the agglomerations consist of Si_2N_2O or Mg_2SiO_4). Since these low density pockets do not appear in the undeformed material and are as well visible in very thick areas of the deformed samples, they are certainly not related to the thinning process of the samples (ion-milling) but rather result from the deformation process.

Samples which were deformed in the high temperature regime ($T > 1\,350$ °C) show extended cavitation at the triple junctions (Fig. 10). Spherical cavities located at triple points and elongated cavities extended into the grain boundary can be detected next to each other. The cavities were found in pure Si_3N_4 matrix material but as well at SiC/Si_3N_4 interfaces. There seems to be no preference for cavitation to occur at either type of interface or triple junction. In some cavitated triple junctions some left over amorphous material could be found (marked in Fig. 10). In some cases where the liquid grain boundary film was thicker, along the whole length of two grains, several pores have been formed within it.

Fig. 10. — BF image of cavities which have formed during deformation in some triple points. (Deformation conditions : Si_3N_4 with 10 % SiC, final temperature 1 440 °C, final σ = 284 MPa, final deformation 7 %). Some left over amorphous phase is marked (marker : 100 nm).

However, not all triple junctions are cavitated. The cavities which were observed are most often located at the triple junction and not further away from the triple point in the grain boundary. The cavities are irregularly distributed in the material.

Samples which were deformed at low temperature ($T < 1\,300$ °C) rarely show spherical cavities isolated at triple junctions. Instead, the adjacent grains are separated by large voids (Fig. 11). In the extreme case, extended microcracks appear (Fig. 12). They propagate along grain boundaries and, when SiC

Fig. 11. — BF image of a sample containing 10 % SiC deformed at low temperature, $T = 1\,300$ °C, $\sigma = 250$ MPa, $\varepsilon = 2.5$ %, showing the separation of grains perpendicularly to their common grain boundary (marker : 50 nm).

Fig. 12. — BF image of a sample containing 10 % SiC deformed at lower temperature, $T = 1\,290$ °C, $\sigma = 250$ MPa, $\varepsilon = 2$ %, demonstrating the spreading of microcracks (→ ←) in the matrix material and at fiber-matrix interfaces (marker : 100 nm).

whiskers are present, as well along matrix fiber interfaces as shown in figure 12. Sometimes the cracks propagate intragranular through the Si_3N_4 grains. This has not been observed for the fibers. The direction of crack propagation changes due to the preference of matrix-fiber interfaces and the crack runs around the fiber. In some cases the fiber itself is cracked, the crack propagating through its cross-section.

After the deformation annealings at 1 200-1 450 °C for maximal 100 hours the interface regions between Si_3N_4 and SiC whiskers were analysed by EELS. Firstly, no oxygen could be detected in the interface. Secondly, careful analysis did not give any evidence that interdiffusion occurred between the two phases, neither carbon in Si_3N_4 nor nitrogen in SiC could be detected. Microdiffraction at the interface does not show any other phase, but without any TEM lattice imaging, the presence of a very thin film cannot be excluded.

Samples which were deformed first at low temperature and later at high temperature show only some large cracks, which means that most of the microcracks healed during annealing at high temperature.

The dislocation density in deformed samples is not much higher than in the original material. Some regions of higher dislocation density which could be detected in some samples can be due to the inhomogeneous distribution of dislocations of the starting material.

Dislocation arrays and strain contrast could often be detected in the matrix at the tips of fibers. This is in agreement with measurements of a residual stress field around the fibers in composites by neutron diffraction [17].

During our deformation anneals sintering occurred, specially at high temperature and for long reaction time. Consequently, some large grains have formed, which are not always dislocation-free. The small surrounding grains remain dislocation-free.

The very inhomogeneous microstructure after deformation at high temperature is shown once more in a SEM micrograph of the surface of a sample which was fractured at room temperature (Fig. 13). Even in the SEM images at very high

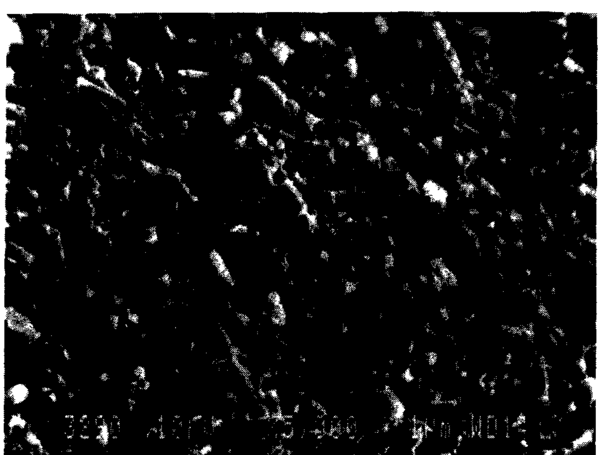

Fig. 13. — SEM micrograph of a sample containing 5 % SiC, which was deformed at high temperature ($T = 1\,500$ °C, $\sigma = 100$ MPa, $\varepsilon = 1.5$ %) and afterwards fractured at room temperature perpendicularly to its deformation axis.

magnification the characteristics of the different temperatures are visible, regions with cavities can be identified in high temperature samples, while possible microcracks in low temperature deformed samples become visible.

4. Discussion.

4.1 INITIAL MICROSTRUCTURE OF THE MATERIAL. — Since the investigated material was hot pressed with an addition of 3 % MgO, the formation of a glassy grain boundary film should be expected. Indeed, this film was observed by electron microscopy, but only in part of the triple junctions and grain boundaries between Si_3N_4 grains. Two reasons might account for this observation : firstly, a very thin glass film may be present in all grain boundaries, which could only be detected by high resolution electron microscopy, a technique which was not available for this study. Secondly, the MgO distribution in the material may be inhomogeneous, which would yield isolated glassy pockets and a partial wetting of the grain boundaries. The analytical identification of the glassy grain boundary phase consisting mainly of amorphous Mg_2SiO_4 is in agreement with observations by Lange, Davis, Clarke [18], who reported a strong dependence of the grain boundary phase composition on the oxygen content of the material, ranging from Mg_2SiO_4 at low oxygen content to Si_2N_2O in more oxidizing atmosphere.

For SiC-containing materials no difference in the microstructural appearance was detected. Both the grain size distribution and the location of the grain boundary phase are similar to those in pure Si_3N_4. At the interface between Si_3N_4 grains and SiC whiskers no glassy film could be detected. The phases seem to be in direct contact and do not diffuse into each other.

4.2 DEFORMATION MECHANISMS. — From the results presented in the preceeding sections (3.1, 3.2) it is possible to identify the deformation mechanisms of pure Si_3N_4 and SiC-whisker reinforced Si_3N_4. The creep behaviour (Tab. I) and the change in the microstructure during deformation (Figs. 10-12) are evidences for a change of the controlling deformation mechanism with temperature. For both types of materials, pure Si_3N_4 and whisker-reinforced Si_3N_4, the low temperature regime extends up to about 1 300 °C and the high temperature regime becomes dominant above 1 350 °C. Our investigation shows that the change from one regime to the other is reversible and does not greatly depend on the applied stress. Our experiments do not allow to decide whether the change in behaviour is abrupt or continuous over an extended temperature range. From now on, these two dominant mechanisms will be referred to as « low temperature » and « high temperature-mechanism » and will be discussed separately.

As a common feature of the two temperture ranges, the dislocations do not play an important role. The few dislocation arrays or centres of high dislocation density observed in deformed as well as undeformed materials, are likely to be residuals from hot pressing or cooling. Consequently, for the whole temperature range investigated here, plastic deformation by a dislocation mechanism can be excluded. This conclusion is in agreement with several other investigations on differently doped Si_3N_4 [15, 18-21].

For the high temperature region, a stress exponent of about 2 was determined together with a formal activation energy of about 7.6 eV/atom. Cavities at triple junctions, or sometimes extending into the grain boundaries, as well as low density pockets, were observed in the deformed samples. The left over glassy phase, which was observed in some cases around some cavities, is an evidence that cavities form within the glassy phase at triple junctions. In most cases no amorphous phase could be proved around the cavities. The observed cavities, separated grains and some strain whorls at grain boundaries indicate a deformation mechanism by grain boundary sliding. As already mentioned above the grain boundary sliding has to be accomodated by some material transport to preserve the structure of the material. A viscous flow of the Si_3N_4 grains within a glassy phase can be excluded, because the amount of glassy phase is not sufficient. Viscous flow with a dissolution of Si_3N_4 in the glassy phase and reprecipitation as main mechanism of the deformation can be excluded because typical related changes in the

microstructure were not observed in our case. As well a pure diffusional mechanism (Nabarro Herring or Coble Creep) as the rate-controlling component of the deformation can be excluded, since in this case the stress exponent should be 1 (not as observed in our case : 2 and above) and typical shape changes of the grains should be visible. A stress exponent of 2 fits well with a mechanism where the sliding is facilitated by the presence of a continuous liquid film in the grain boundaries or at least isolated glassy pockets in the triple junctions and where the grain boundary sliding is accomodated by the formation of grain boundary cavities [6]. The observed microstructure of the deformed samples gives evidence for the formation of irregularly distributed cavities at triple junctions. Cavitation along the grain boundaries, which was not at the triple junction, could not be detected.

In the starting material with its glassy film along grain boundaries viscous sliding can occur. During the sliding of the grains, the fluid phase would be constrained. In particular high tensile stresses would appear at the grain boundaries parallel to the deformation direction. They would cause a negative pressure in the triple junctions and finally lead to a cavitation of the fluid phase. If cavitation has occurred, further material transport in the glassy phase can occur by diffusion in the glassy film itself, by surface diffusion on the walls of the cavity or by transport through the gas phase of the cavity coupled with a evaporation and reprecipitation process. The matter flow results in a propagation of the cavity along the grain boundary.

This deformation process is in agreement with all our microscopy observations at high temperatures. As well the measured stress exponent of 2 is in agreement with calculations of the described mechanism [6]. But it is difficult to estimate an activation energy for this mechanism and compare it with our measured values. Even if we use our EELS analysis, proving that the glassy phase consists mainly of Mg_2SiO_4, and assume that the glassy phase forms a continuous network along all grain boundaries, the data known for the transport in free liquid Mg_2SiO_4 could not be used, because the thin grain boundary film has very different properties compared to the free liquid.

An approximate value of the activation energy for this process might be given by the comparison with ceramics which are characterized by extended grain boundary films. They all show activation energies of about 8 eV/atom, a value which would be in agreement with our observations.

If the glassy phase consists only of isolated phase regions in triple junctions, the cavity formation occurs as described above, but the growth of a cavity will be more complex, because atoms will diffuse partly along the clean grain boundaries and partly through the liquid film. In this complex case, it is even more difficult to estimate an activation energy for the whole process. If the glassy phase is not homogeneously distributed in the starting material, that is localized at some grain boundaries or triple junction, then cavitation and following growth of cavities should be easier, and consequently more dominant in these regions. As a consequence, areas with higher porosity should form. This is in agreement with our detection of exactly what we detected as « low density pockets » for both temperature regimes.

From all the above observations, it is then reasonable to conclude that cavitational creep is the dominant deformation mechanism in the high temperature regime.

At *lower deformation temperature*, more elongated cavities (isolated round cavities at triple junctions are rare), together with low density pockets and microcracks have been observed. The stress exponent was measured as $n = 3.3\text{-}4.5$. The strain hardening coefficient was found to be much higher than for the high tempeature regime.

If we assume once more that the deformation mechanism is grain boundary sliding, it can be easily seen that the liquid film viscosity increases considerably with decreasing temperature, up to a certain threshold temperature where a continuous meniscus can no longer be maintained [9]. In this case the film becomes brittle and fractures along its length. As a consequence, the cavities in grain boundaries become more elongated. In regions where several cavities can interact, elongated microcracks should even form since a relaxation of the stress field at the crack tip by the viscous fluid is not any more guaranteed. This mechanism of microcracking of the glassy grain boundary film during deformation can explain the very high strain hardening coefficient which was found in this temperature regime : the stored deformation energy can be used for fracturing the film and for crack branching, which then becomes possible at all triple junctions. For deformation mechanisms involving microcracking, high stress exponents in a formal power law description have often been reported. This can be due to a change of the rate determining step in the mechanism which compensates viscous sliding. The rate controlling step will definitely not be diffusion, because in this case the stress field around the tips of microcracks would be relaxed by material transport and yield most likely closed cavities.

A simple explanation of the low temperature behaviour by a crystallization of the grain boundary phase, which was liquid at higher temperatures, can be excluded, since the glassy phase should melt above 1 500 °C and consequently be not liquid in any of our experiments.

After the discussion of our results on the defor-

mation in the two temperature regions we want to compare these results reported with those reported in the literature. Many deformation studies have been made with Si_3N_4 containing different additives. Most references are given in the review by Langdom, Cannon [22]. We only want to briefly summarize the major results on MgO fluxed Si_3N_4 : in all these materials an intergranular phase was verified [3-5], which influences the mechanical properties. The deformation behaviour depends strongly on the oxygen content in the sample and the surrounding atmosphere [18]. At high oxygen content the intergranular phase consists of Si_2N_2O. Under these conditions the material is reported to deform by a diffusional mechanism with a stress exponent of 1 and without any formation of cavities. At low oxygen content the glassy film consists of Mg_2SiO_4. In this case Clarke *et al.* found a stress exponent of 2 and extended cavitation [18]. This is in good agreement with our observations for the high temperature regime.

Extended microcracking was observed by N. Tighe during bending tests in air [19], but a comparison with our results might be difficult, because firstly the viscosity of the intergranular phase is a strong function of the temperature and the exact composition, and secondly the local tensile stress for compression creep experiments and bending tests are not comparable.

4.3 INFLUENCE OF THE SiC WHISKERS. — In this last paragraph, our observations on the influence of the fibers shall be discussed. Creep curves and microscopy investigations agree with the fact that whisker reinforcement has no large effect on deformation. The strain rates of pure Si_3N_4 and reinforced Si_3N_4 with 5, 10, 15, 20 % SiC-whiskers (at a given stress) are very similar. As well, stress exponents and strain hardening coefficients show no evident difference. Cavitation and microcracking were observed in all samples, although there might be a slight preference for crack propagation at the fiber-matrix interfaces. This is surprising, because an extended glassy phase could not be detected at SiC/Si_3N_4 interfaces. A strong bridging of SiC fibers across microcracks does not occur, instead the fracturing of the whiskers through their cross-section can be observed if the crack arrives perpendicularly to the interface. This might be due to defects in the particular whiskers.

An extended comparison with results reported in the literature will now be given for Si_3N_4-carbide composites. About ten years ago Birch and Wilshire [21] deformed under compression composites consisting of Si_3N_4 (+ MgO) and SiC particles. They varied the volume fraction of SiC-particles from 0 to 40 vol % and the SiC-particle size from 2 to 50 μm during their experiments. The effect of the SiC addition on the creep behaviour was not marked : for pure Si_3N_4 and for the composite materials a stress exponent of ≈ 2 and an activation energy of 650 kJ/mol were found. Extended crack formation along the SiC-Si_3N_4 interfaces was observed by optical microscopy. Furthermore, a decrease of the creep strength was marked for particle sizes of SiC above a certain threshold value, which itself increases with the volume fraction of SiC. The hot-pressed samples used in this investigation were not completely dense and showed an alignment of the more elongated SiC particles during hot pressing perpendicularly to the compression axis. Consequently, the creep rate of the material was about 3 times larger when the stress was applied perpendicularly to the hot pressing axis than when applied parallel to this axis (due to the possibility of the formation of longer cracks).

Nixon *et al.* [15] compared Y_2O_3/Al_2O_3 fluxed Si_3N_4 without and with 20 % of Sic whiskers (same type of fiber as used in our investigation). They found a similar behaviour of the reinforced and pure matrix materials, with viscous flow being the dominant mechanism (n = 0.5, 0.6). Since they used a high additive content the grain boundary phase partly crystallized during annealing. In their mind the crystallization was much faster in the case of pure Si_3N_4 and became important for the composite at higher temperature, so that the viscous flow was hindered by grain boundary recrystallization. In the microstructure of these materials no triple point voids or grain boundary porosity was observed. Due to the much larger content of glassy phase the results reported [15] cannot be compared with ours. Eventhough, it is interesting to note, that the whiskers do not hinder the viscous flow.

Other investigations performed by Lundberg *et al.* [23] on the flexural strength and fracture toughness of Si_3N_4 containing 0 to 20 % SiC whiskers show even a slight decrease of the strength with increasing SiC whiskers content. For larger fibers with a diameter from 3 to 10 μm, a strengthening of the material was reported [24].

Similar results for the fracture strength are given for a Y_2O_3, Al_2O_3-fluxed Si_3N_4 [25]. The fracture toughness decreases with the addition of small SiC particles (diameter 0.5 μm), while it slightly increases by addition of large SiC particles (diameter 8 μm). For fibers with similar dimensions to ours an increase in strength is observed only at high fiber contents ($\approx$ 30 vol %).

Conclusion.

The mechanical behaviour of a composite consisting of Si_3N_4 with 3 % of MgO additive and 0-20 % SiC whiskers was studied at temperatures between 1 250 and 1 500 °C in compressive creep experiments. The

whiskers play an insignificant role for the deformation. Instead, the intergranular phase which consists of amorphous Mg_2SiO_4 and is located in triple junctions and as a thin film in grain boundaries determines the creep behaviour : two temperature regions could be detected. At high temperatures the materials deform at a quasi-stationnary strain rate by a mechanism of grain boundary sliding with a cavitation of the glassy phase at the triple junctions. At lower temperatures the creep rate becomes much slower, while the strain hardening increases to high values. In this region the deformation occurs still by grain boundary sliding, but since the viscosity of the glassy grain boundary film has decreased under a certain threshold value, the film breaks during the sliding of the grains against each other, leading to a formation of microcracks along the grain boundaries.

All our observations show, that the SiC whiskers do not change the deformation behaviour, neither at high temperatures, nor at low temperatures. Only a slight preference for SiC-Si_3N_4 interfaces during crack propagation was noticed. This can be explained by the fact that no special interphase or enrichment of the glassy phase was observed between SiC and Si_3N_4. Consequently, the interface between the two phases is not specially a « weak » interface, where cracks propagate easily or deformation occurs easier than in the surrounding material. With this knowledge it is not surprising that he composite deforms like the pure Si_3N_4.

By the presence of the harder second phase particles a larger resistance against ductile deformation was expected, with the special hope, that the SiC whiskers would act as obstacles against the deformation. But since the whole deformation is determined by the grain boundary phase, the whiskers do not play the expected role. Some reasons might be found in their dimensions, which are not much larger than those of the matrix grains, and in the whisker content, which might be too low. Longer whiskers or higher whisker content might yield the expected barrier effect.

Acknowledgments.

The authors are grateful to D. J. Rhodes and the Advanced Composites Material Corp. for making the samples available. They thank P. Eveno, J. L. Strudel, R. Molins and B. Pellissier for their assistance in the course of the work. One of the authors (M. Backhaus-Ricoult) wants to thank the Deutsche Forschungsgemeinschaft for a fellowship which made her research at the L.P.M. possible. Another author (J. L. Routbort) is grateful to the French M.R.E.S. for financial support for a stay at the L.P.M. and for the support of the work by the U.S. Department of Energy, Basic Energy Sciences-Materials Sciences, under contract W-31-109-Eng.-38.

References

[1] LANGE, F. F., *J. Am. Ceram. Soc.* **57** (1974) 84.
[2] CLARKE, D. R., THOMAS, G., *J. Am. Ceram. Soc.* **60** (1977) 491.
[3] LOU, L. K. V., MITCHELL, T. E., HEUER, A. H., *J. Am. Ceram. Soc.* **61** (1978) 462.
[4] LOU, L. K. V., MITCHELL, T. E., HEUER, A. H., *J. Am. Ceram. Soc.* **61** (1978) 392.
[5] TIGHE, N. J., WIEDERHORN, S. M., CHUANG, T. J. and MCDANIEL, C. L., *Deformation of Ceramic Materials II,* Ed. R. C. Bradt (Plenum Press) **18** (1984) 587.
[6] EVANS, A. G., RAMA, A., *Acta Metall.* **28** (1980) 129.
[7] RAJ, R., ASHBY, M. F., *Metall. Trans.* **2** (1971) 1113.
[8] DYSON, B. F., *Met. Sci.* Oct. (1976) 349.
[9] TSAI, R. L., RAJ, R., *Acta Metall.* **30** (1982) 1043.
[10] CHANG, K. S., LANKFORD, J., PAGE, R. A., *Acta Metall.* **32** (1984) 1907.
[11] SHALEK, P. D., PETROVIC, J. J., HURLEY, G. F. and GAC, F. D., *Am. Ceram. Soc. Bull.* **65** (1986) 351-56.
[12] BECHER, P. F. and WEI, G. C., *J. Am. Ceram. Soc.* **67** (1984) C 267-9.
[13] SINGH, J. P., GORETTA, K. C., KUPPERMAN, D. S., ROUTBORT, J. L. and RHODES, J. F., *Adv. Ceram. Mater.* submitted.
[14] CHOKSHI, A. H. and PORTER, J. R., *J. Am. Ceram. Soc.* **68** (1985) C144-4.
[15] NIXON, R. D., CHEVACHAROENKUL, S., HUCKABEE, M. L., BULJANAND, S. T., DAVIS, R. F., *Mat. Res. Soc. Proc.* in press.
[16] GERVAIS, H., PELISSIER, B. and CASTAING, J., *Rev. Int. Hautes Temp. Refract.* **15** (1978) 43-47.
[17] ROUTBORT, J., personal communication.
[18] LANGE, F. F., DAVIS, B. I., CLARKE, D. R., *J. Mat. Sci.* **15** (1980) 601, 611, 616.
[19] TIGHE, N. J., *J. Mater. Sci.* **13** (1978) 1455.